

*This is an electronic preprint version of an article published as:*

Onno Wink, Harvey S. Hecht, Daniel Ruijters:  
"Coronary Computed Tomographic Angiography in the Cardiac Catheterization Laboratory:  
Current Applications and Future Developments",  
Cardiology Clinics, (book chapter), Advances in Coronary Angiography, edited by S. J. Chen  
and J. D. Carroll, Volume 27, Issue 3, August 2009, pp. 513-529.  
[doi:10.1016/j.ccl.2009.04.002](https://doi.org/10.1016/j.ccl.2009.04.002)

## Chapter 12

# Coronary Computed Tomographic Angiography in the Cath Lab: Current Applications and Future Developments

Onno Wink, PhD<sup>a</sup>, Harvey S. Hecht, MD<sup>b</sup>, and Daniel Ruijters, MSc<sup>c</sup>

<sup>a</sup>Clinical Researcher, Cardiovascular X-ray, Philips Healthcare, Bothell, Washington, USA

<sup>b</sup>Chief of Cardiovascular Computed Tomography, Lenox Hill Hospital, New York, New York, USA

<sup>c</sup>Senior Scientist, Cardiovascular X-ray, Philips Healthcare, Best, The Netherlands

Keywords: CTA, PCI, coronary interventions, coronary angiography

<sup>a</sup>Corresponding author for proof and reprints:

Onno Wink PhD, Research Scientist

Philips Healthcare/UCDHSC

Interventional Cardiology Section

Leprino Building, Room 510, B-132

12401 East 17th Avenue

Aurora, CO 80045

onno.wink@philips.com (e-mail)

<sup>b</sup>Coauthor address:

Harvey Hecht MD,

Chief of Cardiovascular Computed Tomography,

Department of Interventional Cardiology, Lenox Hill Hospital, 9th floor,

130 E. 77th St., New York, NY, 10021.

<sup>c</sup>Coauthor address:

Daniel Ruijters MSc

Philips Healthcare - X-Ray Predevelopment

Veenpluis 6 - Building QJ2124

5680DA Best - the Netherlands

danny.ruijters@philips.com (e-mail)

Synopsis:

The last couple of years have seen a marked increase in the number of cardiac CT scans performed, regardless of reimbursement issues and concerns about radiation dose. Most major manufacturers are now offering 256+ slice scanners with the ability to ‘cover’ the heart in several rotations and various tools to dramatically reduce the radiation needed to construct a high quality 3D scan of the coronary arteries. This chapter will address some of these recent advances but perhaps most importantly will discuss avenues of how the CT and its derived information can be used in the preparation and execution of a diagnostic cath and a PCI, once the decision is made to intervene.

## 12.1 Introduction

The last few years have seen a marked increase in the number of cardiac CT scans performed, regardless of reimbursement issues and concerns about radiation dose. Most major manufacturers are now offering very fast 256+ slice scanners with the ability to ‘cover’ the heart in several rotations and various tools to dramatically reduce the radiation needed to construct a high quality 3D scan of the coronary arteries. While studies consistently show the very high (upper nineties) negative predictive value (or the absence of disease) based on CT [Hecht07,Meijboom08] the ability to precisely define coronary artery disease has varied, leading to the common perception that CTA cannot adequately deal with complex CAD [Hendel06]. However, recent advances, as well as the appropriate use of commonly available analytic tools, permit the extraction of the remarkable data offered by this technology and show its potential to have an impact on planning both the catheter coronary angiography (CCA) and the percutaneous coronary intervention (PCI) performed in the cardiac catheterization laboratory, as will be discussed in this chapter.

## 12.2 Advances in coronary CTA acquisitions

The latest generation of CTA scanners provide increased coverage (8 cm to 16 cm/ rotation) and shorter acquisition times. The newer 256 (Philips) and 320 (Toshiba) slice scanners decrease the likelihood of patient motion, respiration and heart rate variations that degrade image quality [Motoyama08]. In addition improved temporal resolution is associated with faster rotation speeds (Philips) while dual source imaging (Siemens) minimizes motion artifacts. Improved spatial resolution provided by new detector technology (General Electric) can be expected to improve image quality. Another area, currently under development is ‘dual energy imaging’ aimed to minimize the effects of calcified plaque, or potentially allow for a distinction between types of plaque. Apart from this continuous development in the hardware, smarter acquisition protocols and improved injection profiles have dramatically reduced the amount of radiation and the quality of the reconstructions. As an example, the prospective, “step and shoot” axial imaging with radiation applied only during a mid-diastolic phase decreases the delivered dose to as low as  $4.3 \pm 1.3$  mSv, with sensitivity of 96.4%, specificity of 98.5%, and a diagnostic study rate of 96.6% [Takada06]. By combining more intelligent acquisition protocols and improved hardware capabilities, some manufacturers predict a complete diagnostic study with less than 2 mSv in the not too distant future.

### **12.3 Reviewing coronary CTA**

After reconstruction, the CTA volume is sent to a digital workstation for further processing and to allow detailed analysis of the coronary arteries. This section will give details of common segmentation and extraction techniques of the areas of interest from the CT datasets, and will discuss different visualization techniques that can be used to aid the reviewer in arriving at a proper diagnosis and an appropriate assessment the extent of the patient's coronary disease.

#### ***Basic reviewing tools***

In the unprocessed (or raw) CT image data the three dimensional volume consists of volume elements or voxels. Each voxel's intensity is based on its corresponding Hounsfield unit, reflecting its radiopacity. Routine review of the CT by browsing through the axial images (consisting of only one layer of voxels) allows for a quick scan for potential disease, but does not allow for sophisticated data extraction. The next step for the user is to freely define a set of cross sectional planes that 'cut' through the CT volume with a slab thickness that can be varied. Within the slab, the maximum intensity projection (MIP) technique is utilized to display the brightest voxels. The operator has the freedom to create multiple oblique rotations of these slabs. The latter technique is the most common analytic method, primarily because it requires virtually no post processing. The propagation of this technique has negatively affected CTA interpretation by rarely displaying the entire vessel in a single image, and by not providing the platform for crucial cross sectional analysis. In addition, incorrect slab thickness is a common error. If the slab thickness is less than the diameter of the coronary artery it may not show significant calcifications. On the other hand, if the slab is set too thick, it may highlight adjacent high intensity voxels that do not belong to the current vessel of interest and may mask significant stenosis.

#### ***Advanced viewing tools***

More detailed analysis of the cardiac CT dataset requires the (semi-)automatic extraction of the regions of interest. Typically, the first step in any automated analysis or processing of cardiac CT images is the segmentation of the heart. During the segmentation process the individual voxels are assigned to a certain anatomy or to the background. Depending on its purpose, the segmentation step will try to identify several cardiac structures [e.g. Okuyama08,

Spoeck08, Cristoforetti07, Sun05, Lynch06], or the whole anatomy of the heart [e.g. Zheng08, Ecabert08, Wijesooriya08, Fleureau07, Renno06, Lorenz06, Assen08, Cho05].

Segmentation algorithms can be divided into two classes: model-less and model-based approaches. The approaches of the former class typically consist of a chain of basic image processing operations, such as thresholding, region growing, edge detection, etc. and often require some form of user interaction (e.g. placing seed points) [e.g. Higging90, Redwood05]. These methods can be time consuming and are prone to operator bias. The algorithms in the model-based class extract the most descriptive statistical properties from a large pre-annotated training database or otherwise build an atlas based on this training set. The segmentation algorithm then tries to fit the model to a given dataset by varying the parameters of the model according to the predetermined statistical range. Most of these model based approaches first perform a rough estimate of the location of the heart, and then adapt a generalized model to the specific patient data by locally deforming the model. After the heart has been identified, the main anatomical structures, such as the atria, ventricles, myocardium and large vessels, are segmented. In the last few years, these methods have matured both in terms of reliability and processing time, making them the method of choice for most digital workstations. Figure 1 shows an example of a fully automatic segmentation of a CTA volume in the most basic cardiac structures.

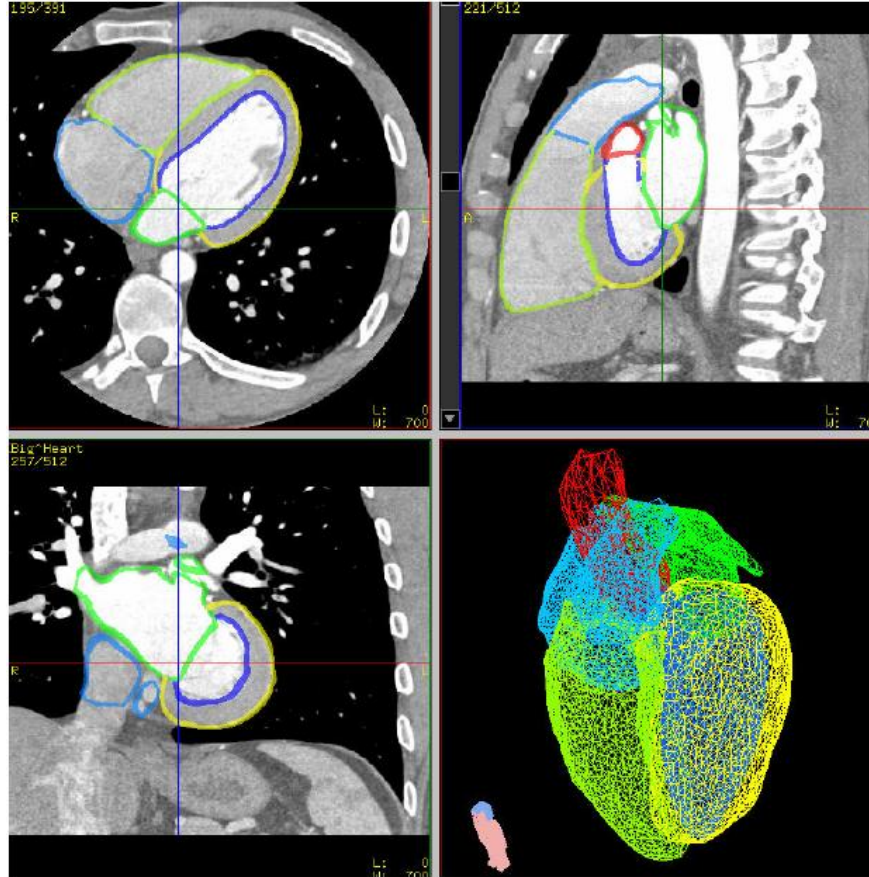


Figure 1: Example of model-based fully automatic segmentation of the main cardiac structures from a CTA dataset. The extracted 3D surface mesh or model of the different structures is shown in the right lower frame, while it is also superimposed on the three orthogonal slices in the cardiac CT volume.

A disadvantage of these model based approaches is that it may have difficulties dealing with anomalies and/or congenital deformities since the underlying model is not trained in these variations of the anatomy. In practice, this generally implies that the user is given the option to revert back to semi-intelligent manual (model-less) segmentation tools to handle these challenging cases. Regardless of the approach, the minimum segmentation should yield an effective extraction of the voxels that belong to the heart and its surrounding structures. Effectively, the spine, ribs and other structures should have been removed. An example is given in Figure 2, in which a lookup table is applied based on the Hounsfield values to make the visualization of the heart appear more ‘realistic’.

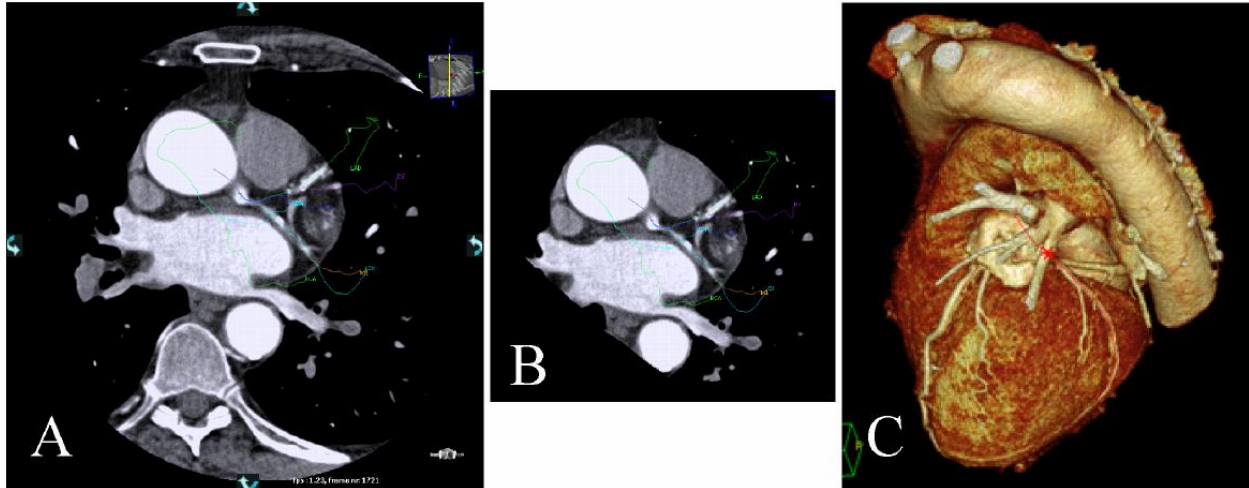


Figure 2: Example of the segmented heart from a CTA volume. A slice from the original CTA scan (A), the same slice after segmenting the heart (B), and a color coded volume rendering of the segmented heart (B).

### *Extracting the coronary arteries from the CTA*

The increased spatial and temporal resolution of multi-detector CT has brought imaging and analysis of the coronary arteries within reach [Marquering05, Soaur08, Isgum07, Horiguchi07]. In order to enable automatic analysis of the coronary vessels, they need to be segmented from the CT data as well [Bousse06, Fallavollita06, Fallavollita08, Mueller08, Zambal08]. The extraction of the coronary arteries from the cardiac CT data is generally started after the whole heart segmentation has been performed since it can provide clues of the location of the coronary arteries. The first step consists of extracting the tubular structures in the raw CT data. To facilitate this extraction process a separate representation is often generated in which the vessel-like structures are highlighted. An example of such a ‘vesselness’ [Frangi98] filtered image is shown in Figure 3.

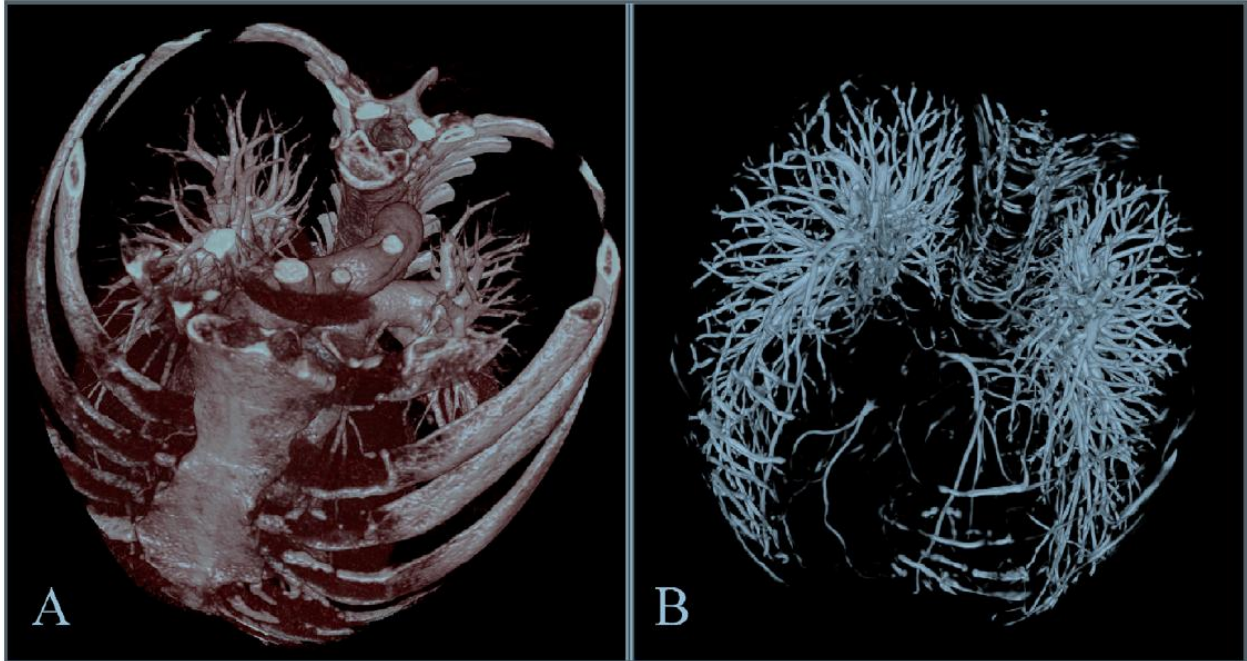


Figure 3: Example of a vessel enhanced image. The left frame shows the original CT data. The right frame shows the same dataset after a vesselness filter was applied. In the center of the volume some of the major coronary arteries are visible.

The coronary artery tree is then traced in the vessel enhanced data, starting at the ostia, which could have been located during the preceding whole heart segmentation. The segmentation algorithm will try to follow the enhanced structures until it reaches a point where it is unsure where to continue. Most commercial packages are capable of extracting the major coronary arteries, but leave it up to the operator to provide the appropriate label. Again, it is always possible to edit and extend the automatically found centerlines or to trace the vessels completely manually.

#### ***MPR's, volume rendering and quantitative tools***

Once the dataset is segmented and the coronary arteries extracted, there are a large number of tools available for visualization of the results. The most commonly used tools are the volume rendering (VR, see also right frame of Figure 2) and the multi-planar reformats (MPR's). The volume renderings generally give an overview of the anatomical location of the arteries and their relation to other vessel structures. Highly calcified regions can also be marked to show the extent of the lesion. As stated earlier, the often tortuous nature of the vessels do not allow them to be captured in their entirety in a single 'cut' through the volume even with a large slab size. This is the main

reason for the existence of the family of MPR's. Figure 4, gives an example of different types of MPR's and the derivation of some quantitative results.

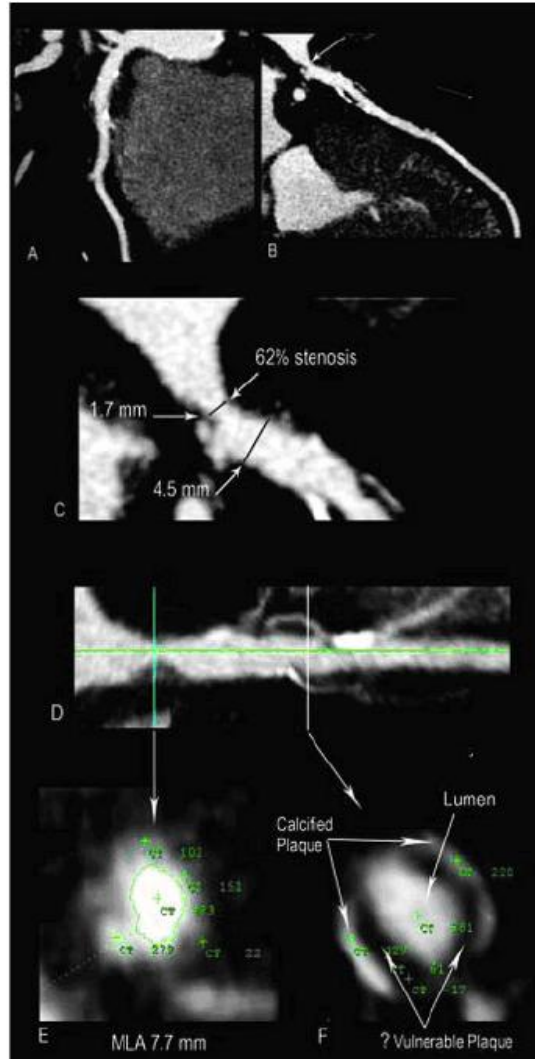


Figure 4: Example of different MPR's and Quantitative CTA analysis.

(A) Left anterior oblique and (B) right anterior oblique CTA multi-planar reconstruction of the left anterior descending coronary artery demonstrating significant stenosis apparent only in (B). (C) Quantitative measurement of the stenotic area in (B). (D) Straightened multi-planar reconstruction with cursors drawn through the proximal stenosis and the more distal complex plaque. (E) Cross sectional analysis of the proximal stenosis. The numbers represent the Hounsfield units of the pixels marked by the adjacent plus signs. The contour is drawn around the

lumen on the basis of the gradation of Hounsfield units. The luminal area within the contour is calculated by the computer program. The measurement of 7.7 mm<sup>2</sup> is more than adequate, (F) Multiple tissue densities are demonstrated, including very low and negative density non-obstructive plaque, with negative Hounsfield units suggestive of a potentially vulnerable thin cap fibroatheroma.

The curved and straightened MPR [Kanitsar02] of the entire coronary artery as shown in Figure 4 are the unequivocal format of choice and should be an absolute requirement. However, total reliance on computer generated MPR's is an invitation to error; center line review and correction by an experienced CT angiographer is essential. The operator must also be aware of the dependence of the diagnostic accuracy on the window center and width settings. Furthermore the quantitative analysis of lesion characteristics is essential (Figure 4c), and vastly preferable to the "eyeball" estimation routinely applied to catheter coronary angiography (CCA). Rotation of the MPR's around the extracted coronary center line allows the operator to display the smallest diameter and to choose a normal reference area devoid of the positive remodeling that accompanies diseased segments and permits more meaningful calculations of % diameter stenosis (Figure 4a-c). The derived % diameter stenosis should be rounded to the encompassing quartile, e.g., 50-75% since the spatial resolution of CTA does not permit more precise quantitation. More importantly, the minimal luminal area (MLA) should be calculated from a cross section derived from the straightened MPR (Figure 4 d,e) based upon gradients from the contrast to the surrounding densities. MLA cannot be derived in sections with calcified plaque contiguous to the contrast. Hounsfield unit interrogation of different tissues may permit identification of negative density lipid adjacent to the lumen that characterizes the thin cap fibroatheroma (Figure 4f).

#### **12.4 The predictive value of CTA and comparison with CCA and intravascular ultrasound**

Although there are a large number of segmentation and visualization tools available, it is not advisable to rely on a single representation and set of preset parameters. The accuracy of CTA is dependent on a highly variable learning curve for achieving adequate processing and interpretative skills; A large number of studies have investigated the use of CTA to predict the absence or occurrence of significant coronary artery disease. Overall, these studies have consistently shown a negative predictive value (vessels do not show signs of significant coronary artery disease) in the 95-99% range [Hecht08], while the positive predictive values are more variable and are

dependent on the disease prevalence. A recent prospective multicenter multivendor study on the use of 64 slice CTA in patients with stable or unstable angina [Meiboom08] made a distinction between patient-based, vessel-based and segment-based performance and showed very impressive results for the negative predictive value in all analyses (see also Table 1), with declining positive predictive values as the disease prevalence decreased.

<b>Level of Analysis</b>	<b>Prevalence of Disease</b>	<b>Sensitivity</b>	<b>Specificity</b>	<b>Positive Predictive Value</b>	<b>Negative Predictive Value</b>
<b>Patient-based</b>	68%	99%	64%	86%	97%
<b>Vessel-based</b>	26%	95%	77%	59%	98%
<b>Segment-based</b>	9%	88%	90%	47%	99%

Table 1: Diagnostic performance of 64-slice CTA, constructed by Caitlin E. Cox based on [Meiboom08], used with permission from TCTMD.

The major concern with regards to most of these comparative studies is the choice of the gold standard. Traditionally, all the noninvasive diagnostic technologies, including nuclear cardiology, stress echocardiography, magnetic resonance imaging (MRI) and positron emission tomography (PET) perfusion imaging, have used a >50% diameter stenosis on CCA as the gold standard, despite the limitations inherent in two-dimensional (2D) lumenology, clearly demonstrated by intravascular ultrasound (IVUS). The most important limitations are: inability to define normal reference areas, limited number of acquisitions, and reliance on percentage diameter stenosis rather than minimum luminal area (MLA). Nonetheless, CCA has also been used as the gold standard for CTA, even though CTA has more in common with IVUS (see also Table 2). In particular, the ability to calculate minimal luminal area ([Cassin06, Okabe08]), to view a stenosis from an infinite number of angles and to characterize plaque ([Pundziute08, Springer08, Pundziute08b]) are IVUS characteristics that impact greatly on PCI. The spatial and temporal resolution of CTA are not likely to improve significantly in the near future but do not diminish its utility. Moreover, the noninvasive, and far less expensive acquisition, as well as the decreasing radiation offered by prospective imaging, are distinct advantages. Although not a coronary imaging tool, myocardial perfusion imaging is associated with more radiation (11-23 mSv) [Thompson06], and is still recommended before CTA in the diagnostic paradigm despite its inferior sensitivity and specificity for detecting significant obstructive disease [Fleischmann98].

	CCA	IVUS	CTA
<b>Spatial resolution</b>	200 microns	100-150 microns	350 microns
<b>Temporal resolution</b>	5-10 ms	NA	40-100 ms
<b>Imaging</b>	Projection / 2D Lumen	Cross sectional Wall and lumen	Cross sectional Wall and lumen
<b>Parameter</b>	% diameter stenosis	Minimum luminal area	Minimum luminal area
<b>Plaque Character</b>	Not applicable	Readily available	Readily available
<b>Imaging area</b>	All segments	Limited segments	All segments
<b>Acquisition</b>	Invasive	Highly invasive	Noninvasive
<b>Radiation</b>	5 mSv	>5 mSv (part of PCI)	2-20 mSv
<b>Cost</b>	High	High	Low

Table 2: Comparison of CCA, IVUS and CTA

### 12.5 Peri-operative use of CTA

If the findings on the CTA result in the decision to proceed with the cardiac cath, then the challenge becomes transferring the information gathered thus far to aid in the decision making process . This section will discuss some options and requirement of the in room use of the CTA data beginning with basic utilization and concluding with future applications.

#### *Adapting the diagnostic catheterization*

In general a complete diagnostic catheterization will be performed regardless of the CTA findings, if only to confirm these and obtain information that is not readily present in the CT scan, such as the assessment of flow and the presence of collaterals. However, the CT data may suggest a series of C-arm angles that may be different than the routine views commonly employed by the cardiologist. Depending on the familiarity of the physician with the CT data and the quality of the scan, an even larger deviation from the routine standard views may be employed. On the extreme end, the entire diagnostic catheterization may be, completely guided by the CT. In this patient specific application, the CT will dictate the viewing angles or (dual-axis) rotational acquisitions that would optimally yield

the vessel segments of interest. Apart from confirming the diagnosis based on CT, it will offer potential working views to perform the actual intervention. In addition, the amount of time, contrast and radiation needed to complete the diagnostic scan, may be reduced as well. In the future, the cardiologist may even refrain from injecting the right coronary altogether if the CTA only shows disease in the left coronary system.

### ***In room visualization and manipulation***

In the anticipation that the CTA will play a more dominant role in the future, several companies have products available or are planning functionality that facilitates the transfer and the utilization of the CT data and some of its quantitative information in the cath lab (e.g. Shina Systems, Siemens, GE, Philips). Especially for complex vasculature, chronic total occlusions (CTO), unusual anatomy and strange take-off angles, it has been shown to be beneficial to have the CT available in the room [e.g. Mollet05, Garcia07, Hecht08, Otsuka08]. Since the ability for in-room manipulation of the CT data and its derived information by the interventionalist during the diagnostic and PCI portion is limited, it is key to show the essentials of the CT information during the critical portions of the procedure. An example is given in Figure 5.



Figure 5: In room presentation of CTA data using volume rendering and MPR visualization techniques.

In Figure 5 a combination of volume rendering and MPR's are shown, specific for the lesion of interest. If a segmentation of the CT into different tissue types (e.g. blood, muscle, bone) and or anatomical segments is performed (e.g. spine, ribs, cardiac chambers), this information can be used to better reveal the areas of interest. From the table side the operator has the opportunity to select the coronary artery of interest and define the vessel segment of interest using sliders. In the lower left panel the C-arm configuration is shown that corresponds with the current viewing angle of the CT dataset. The color coded rectangle on the left middle panel shows the foreshortening map combined with an overlap map (see also chapter [?]), which can other properties to aid in finding the optimal working view for the actual intervention.

Furthermore, a particular X-ray view can be simulated based on the segmented CT data using digitally reconstructed radiographs (DRR). Advances in graphical processing unit (GPU) programming and computing power allow for extremely fast rendering times of these DRR's [e.g. Russakoff05].

Figure 6 gives an example of such a simulated view, where, purposefully the bony structures and the coronary tree as derived from the CT are shown. An advantage of this type of rendering technique is that it displays the data in a fashion more familiar to the interventionalist.

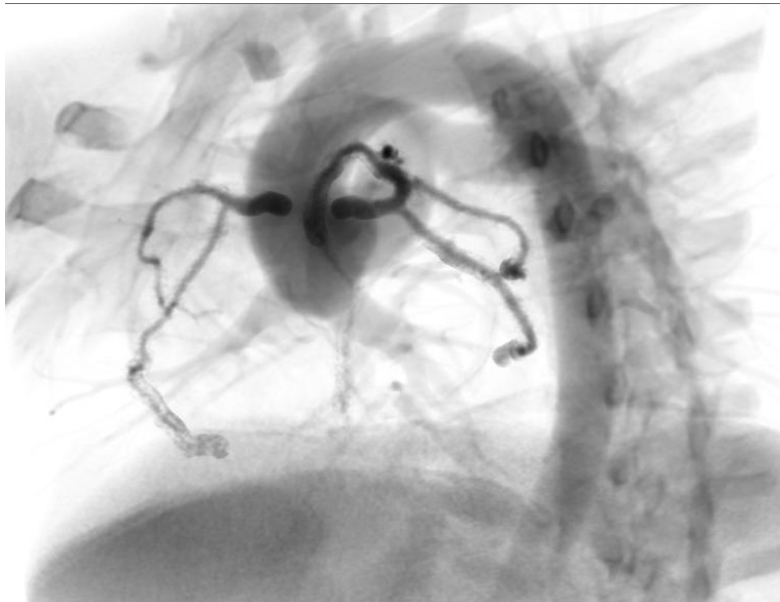


Figure 6: Example of a digitally reconstructed radiograph (DRR) based on a segmented CTA dataset.

Recently, some researchers and manufacturers have moved towards an even more intimate integration of the X-ray acquisition equipment and the pre-operative 3D dataset. As a first step, the C-arm angles of the X-ray gantry are communicated to the 3D workstation to allow the CT to be viewed in the corresponding viewing direction. In these types of applications, the clinician has the opportunity to manipulate the C-arm around while the CT will rotate accordingly. Figure 7 shows an example of the CT rendered coronary tree from several different viewing angles and their corresponding gantry configuration.



Figure 7: Example of visualizing the CT based coronary tree from different viewing angles and the corresponding C-arm gantry configuration.

As an alternative, some systems allow the physician to select a viewing angle solely based on the optimal view map and have the computer proceed to the corresponding viewing angle. The disadvantage of the latter solution, however, is that it may not be feasible to reach the computer generated viewing angle because of the patient dimensions, steepness of the viewing angle and other complicating factors that are less likely to happen when the CT viewing angle is coupled with the X-ray gantry.

As a second step, the exact gantry configuration including the table position, height, detector size, source to detector distance (SDD), etc, are communicated. In these applications the configuration of the X-ray gantry is known in real time and used to simulate very impressive accurate renderings of the coronary vasculature that are close to the actual X-ray images. These renderings now take into account the actual gantry configuration such as viewing angles, detector size, source to detector distance (SDD), the table height and translation and even the actual shape of the X-ray beam, resulting in a view with an inversed perspective.

### ***Image fusion***

Future significant advances will require actual fusion of the CTA and CCA images, thereby eliminating the persistent problem of exactly translating a CTA directed intervention to the CCA defined coronary artery. CTA has the potential to be used for roadmapping, by which the stream of live X-ray images are superimposed on the volume

rendered representation of the (segmented) CTA. Although the presumed benefits of these roadmapping applications are currently under investigation, they will likely prove to be crucial for more accurate stent placement and in the treatment of chronic total occlusions, as will be discussed below.

### ***Registration***

In these types of applications it is essential that the CTA dataset is put into the same coordinate frame as the X-ray gantry. In this iterative process, known as the registration process, the anatomical features that are apparent in both modalities are used to compensate for the difference in patient orientation. Typically a registration algorithm consists of a similarity measure, indicating the quality of a given spatial mapping, and an optimization algorithm, which iteratively searches the optimum of the similarity measure. Currently most of these roadmapping applications use either bony landmarks such as the ribs and spine, the pulmonary veins, or the contrast filled coronary arteries, and some approaches make use of the DRR's again to measure the fit between the fluoroscopy images and the CT data [e.g. Weese97]. However, since most CT's are equipped with a concave table, it is not always possible to perform this registration using a simple rotation and translation, and more computationally expensive non-affine registration methods are utilized.

CT – X-ray image registration has a number of clinical applications, such as radiotherapy planning and verification, surgery planning and guidance, and minimal invasive vascular treatment in peripheral and neurovascular interventions. In the cardiac domain, most work with respect to roadmapping applications has focused on electrophysiological interventions [e.g. Sra07, Knecht08], and only recently the possibilities for coronary artery disease treatment are being explored [e.g. Turgeon05, Garcia07, Garcia08]). Although the roadmapping applications based on pre-operative CT and MR have yielded impressive accuracy and several applications in neuro-vasculature and peripheral interventions, its application for performing coronary interventions is challenged by cardiac and respiratory motion. In addition, to salvage the earlier registration the catheterization laboratory table requires a sensor to track its position or an automatic registration process is needed. Figure 8 shows an example the result of an automatic registration technique on a patient's dataset, highlighting some of the challenges.



Figure 8: Example of a registration based on the coronary arteries.

In some experimental settings the use of in-room CT-like reconstruction techniques based on rotational X-ray acquisitions as explained in chapter [?] can be used. The advantage of the latter approach is that there is no explicit need for an image-based registration. Regardless of these issues, image fusion shows great promise, particularly in complex interventions in which the CT data adds complementary information to the X-ray images.

## 12.6 Current and Future Applications of Coronary CTA to PCI

In the previous section, the technology and tools that are currently available (or under development) to the interventionalist were discussed. This section gives some practical examples of how some of these tools can be applied and how they have the potential to impact the treatment plan and the execution of the PCI after a ‘positive’ CT is found.

### *PCI patient selection and identification of significant lesions*

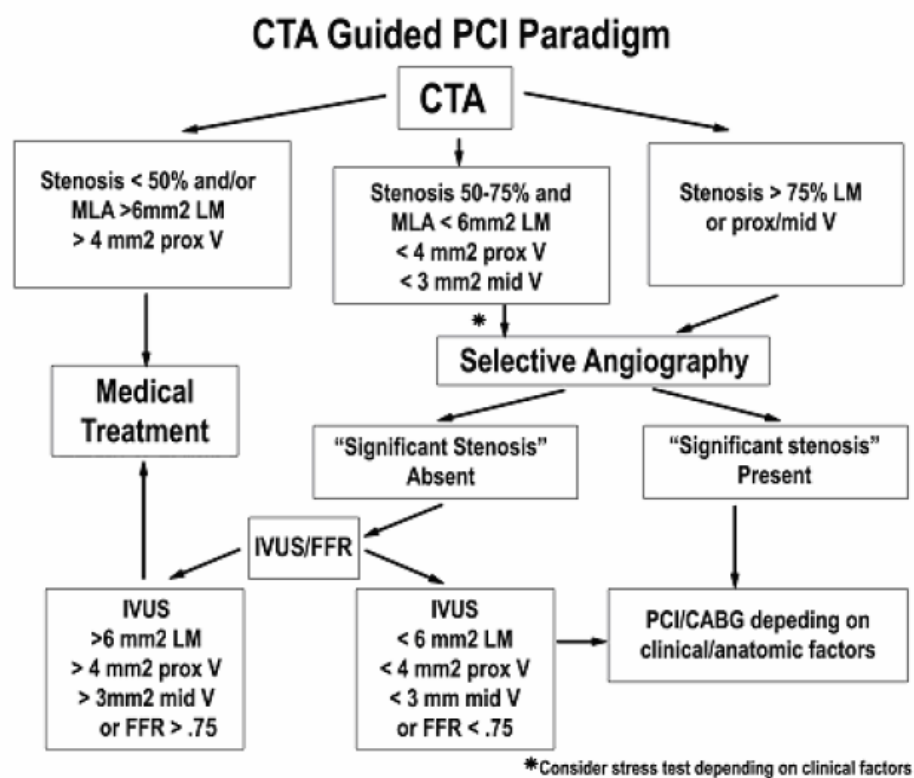


Figure 9: CTA guided PCI paradigm. Abbreviations: CABG= coronary artery bypass grafting. CTA= computed tomographic angiography. FFR= fractional flow reserve. IVUS= intravascular ultrasound. LM= left main. MLA= minimum lumen area. PCI= percutaneous coronary intervention. V= vessel.

The paradigm as shown in Figure 9 [Hecht08] replaces stress testing with CTA as the first test in the evaluation of the CAD patient, and relies more on IVUS minimum luminal area criteria than percent diameter stenosis.

Discrepancies between CTA and CCA stenosis characterization are adjudicated by either IVUS or fractional flow reserve [Tobis07]. In Figure 10 diffuse narrowing of the entire proximal LAD was evident on CTA, with an MLA of 2.9 mm<sup>2</sup>. CCA revealed only minimal narrowing, highlighting its difficulty in identifying diffusely narrowed segments that, by definition, have no normal reference areas. IVUS clearly corroborated the CTA findings [Hecht08],

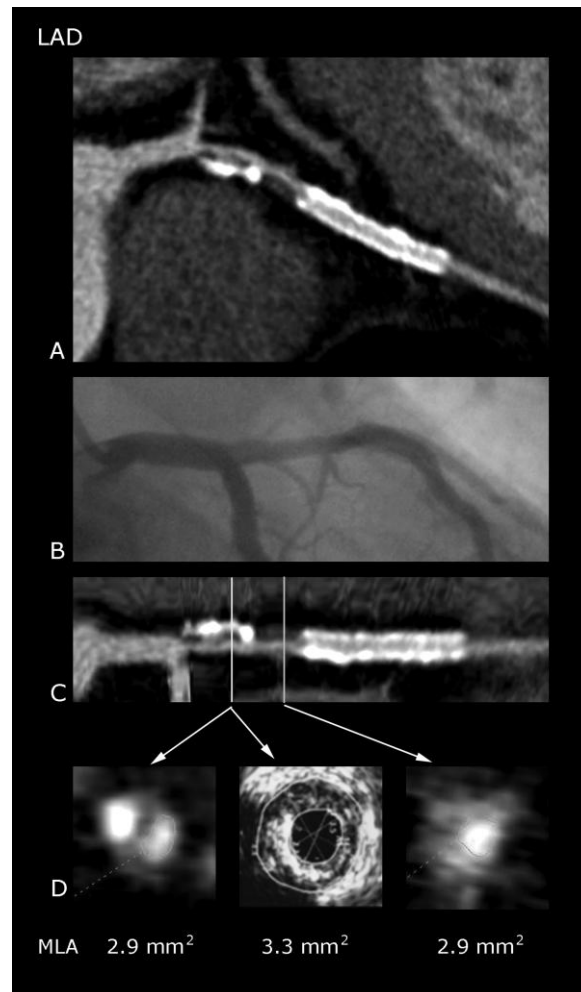


Figure 10: In a symptomatic 64 year old male with prior LAD stent, CTA curved MPR of the LAD (A) revealed significant diffuse narrowing from the LAD ostium to the stent, with only mild narrowing evident on the corresponding CA (B). Cross sectional analysis (D) of the straightened MPR (C) demonstrated significantly reduced MLA of 2.9 mm<sup>2</sup>, confirmed by IVUS (D), and followed by PCI.

Abbreviations: CA= catheter angiography LAD= left anterior descending. CTA= computed tomographic angiography. MLA= minimum luminal area. MPR= multi-planar reconstruction. PCI= percutaneous coronary intervention.

The same principle applies to in-stent restenosis. In Figure 10, uniform in-stent contrast density indicates absence of significant neointimal hyperplasia. Severe in-stent hypodensity is noted in Figure 11, consistent with significant narrowing, not apparent on CCA but confirmed by IVUS [Hecht08].

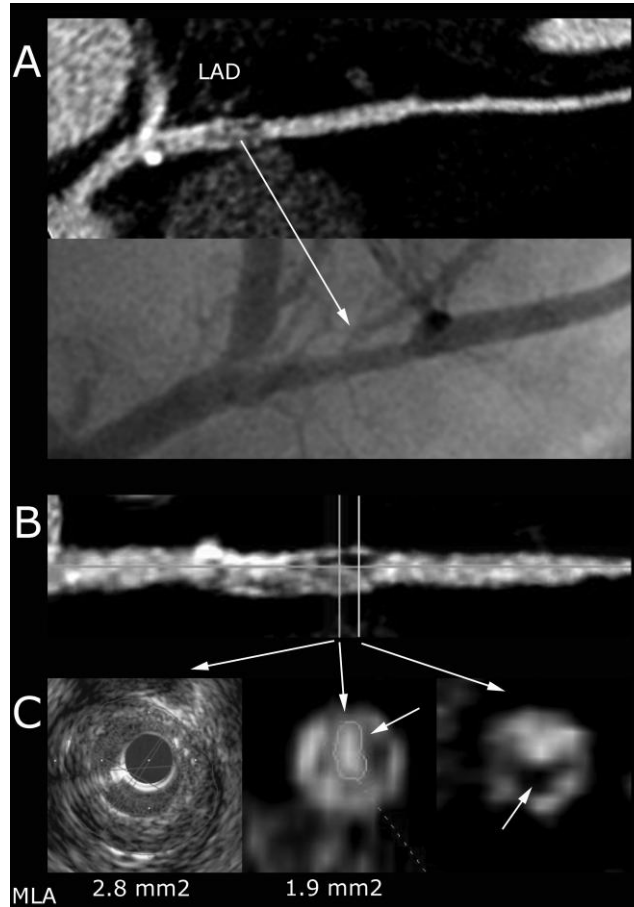


Figure 11: An 80 year old female with increasing dyspnea and prior LAD stenting was evaluated. CTA revealed severe hypodensity consistent with significant in-stent restenosis (A, top) that appeared to be only moderately severe on CA (A, bottom). Cross sectional analysis (C) of the straightened MPR (B) in 2 adjacent areas of the stent demonstrated the hypodensity characteristic of neointimal hyperplasia (arrows), as well as severely decreased MLA, confirmed by IVUS (C). PCI was performed. In-stent MLA calculation is rarely possible. Blooming artifact from the dense stent material almost always precludes accurate measurement; ISR is diagnosed by qualitative density levels.

Abbreviations: CA= catheter angiography CTA= computed tomographic angiography IVUS= intravascular ultrasound LAD= left anterior descending MLA= minimum lumen area MPR= multi-planar reconstruction

***Procedure planning: Stent sizing***

CTA facilitates precise determination of the area to be covered based on measurement of the length of diseased vessel wall that warrants exclusion rather than upon an estimation of the lumen stenosis length on CCA. Proximal and distal landing zones can be axially sized and post dilation planned, as in Figure 12. The angle of least foreshortening of the stenosis can be selected by TrueView (Philips). Presumed vulnerable low density plaques on the stenosis margins may be covered as well, even though there are no supporting data.

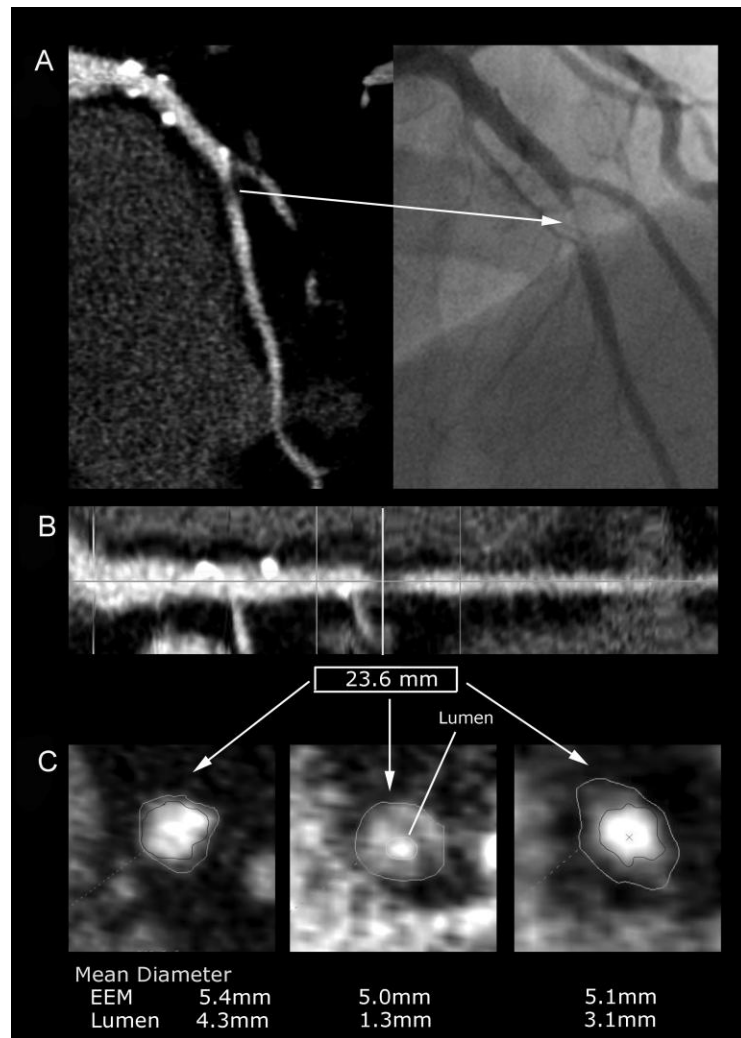


Figure 12: In a 66 year old male with increasing angina, subtotal LAD occlusion (arrow) was noted on the CTA (A, left) and on the CA (A right). Proximal and distal stent landing zones, 23.6 mm apart, were chosen on the straightened MPR (B). Mean luminal diameters for the landing zones were determined by cross sectional analysis to

be 4.4 and 3.1 mm, respectively (C). PCI was performed using a 25 mm x 3.5 mm stent, with post inflation of the proximal segment to 4.5 mm to achieve full apposition.

Abbreviations: CA= catheter angiography CTA= computed tomographic angiography IVUS= intravascular ultrasound LAD= left anterior descending MPR= multi-planar reconstruction PCI= percutaneous coronary intervention

***Procedure planning: Chronic total occlusions***

CTA has long been used for PCI of CTO's [Mollet05], and has been invaluable in identifying the often angiographically invisible occluded segment, which can **always** be tracked by CTA. Of equal importance is pre-procedural determination of the best angle to approach the CTO, using branch vessels as landmarks, as demonstrated in Figure 13.

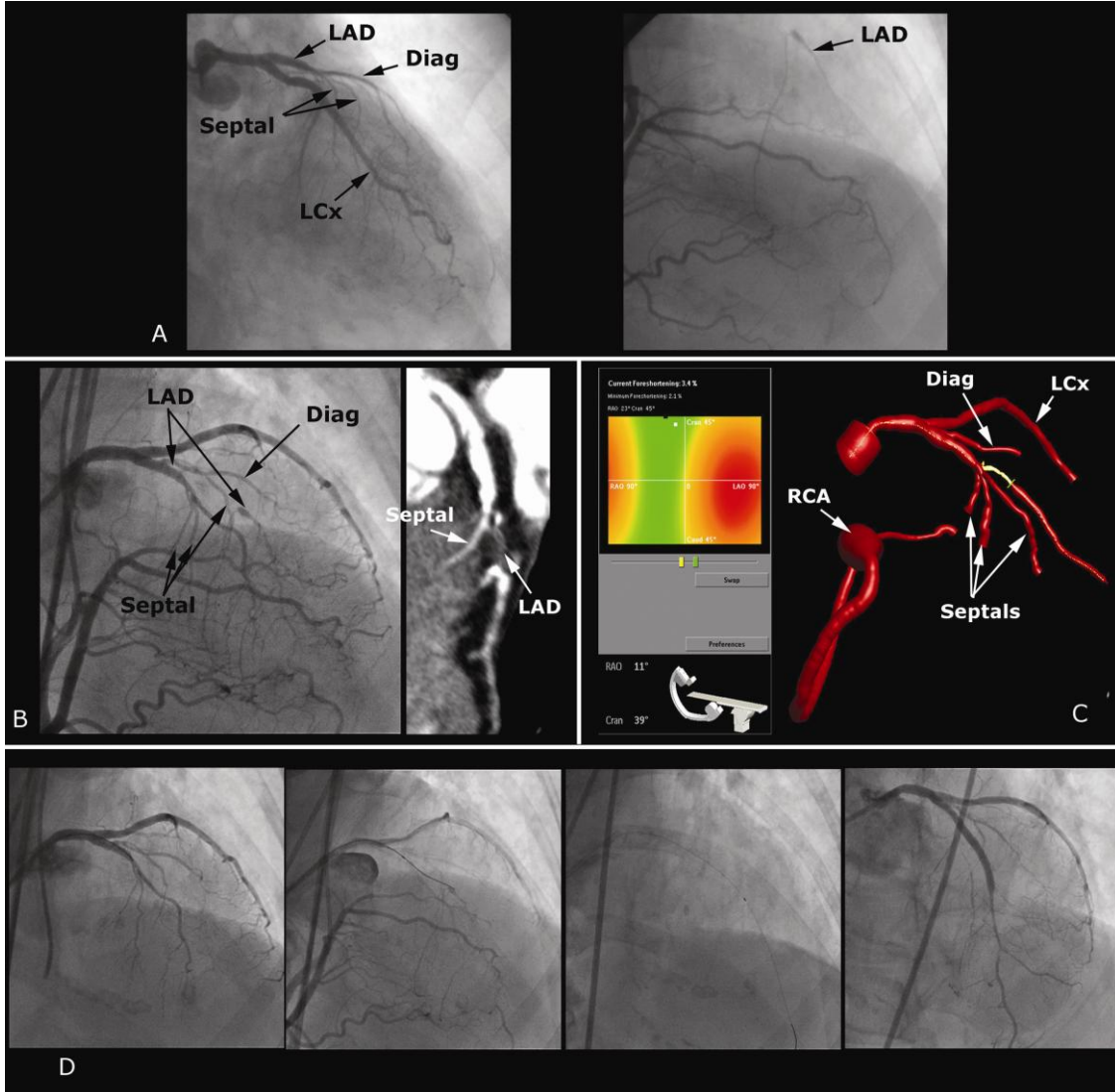


Figure 13: Selective angiography demonstrated flush occlusion of the LAD with partial collateral filling from the RCA (A) in a symptomatic 65 year old woman with anterior ischemia. After 6 months of persistent symptoms, CTA guided intervention was planned. Curved MPR readily visualized the occluded LAD segment (B). CTA mapping (TrueView, Philips) of the left coronary artery and all its branches (C) was imported to the catheterization laboratory monitor and electronically linked to the C-arm. The C-arm was rotated, with accompanying automatic rotation of the TrueView map to the angle predetermined by the CTA to best demonstrate the origin and course of the chronic total occlusion without overlapping branches. Simultaneous injection of the right and left coronary arteries (D) was performed. With TrueView guidance, the guidewire was introduced to the precise origin of the flush occlusion, followed by successful recanalization and further stenting of the distal vessel 6 weeks later (E)

Abbreviations: CTA= computed tomographic angiography    diag= diagonal    LAD= left anterior descending  
 LCx= left circumflex    MPR= multiplanar reconstruction    RCA= right coronary artery

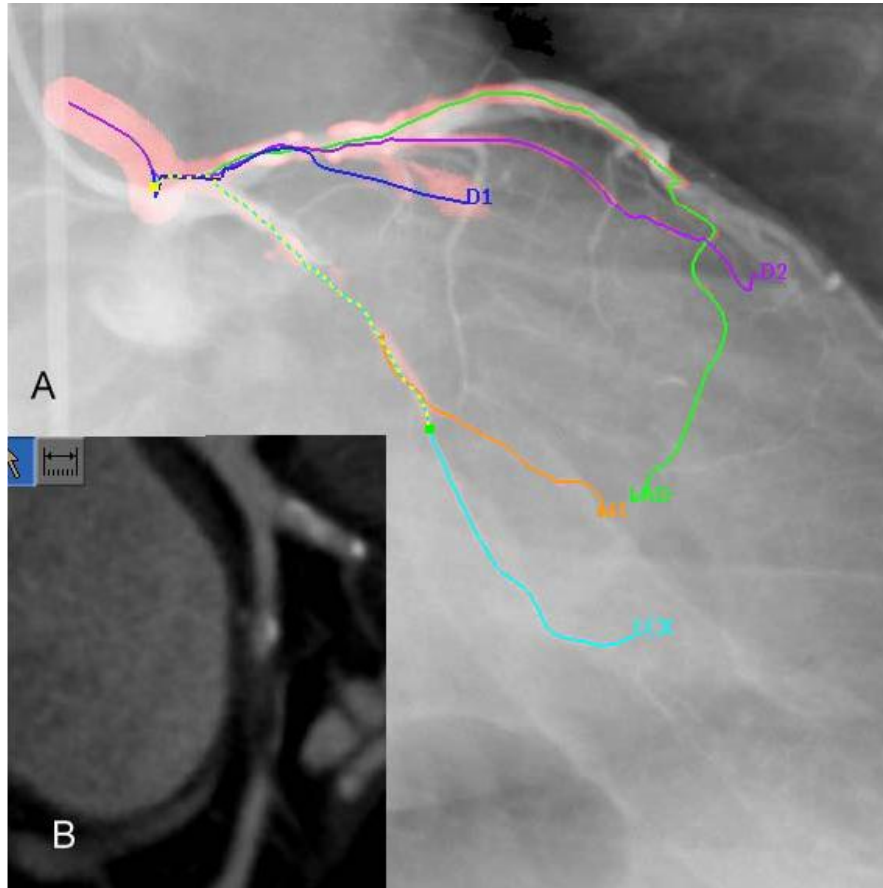


Figure 14: Fusion of CT and X-ray images (roadmapping) A and the corresponding MPR (B).

Figure 14 demonstrates a CTO revascularization using image fusion. The CCA reveals the vessel cutoff, while the superimposed CT images from a similar viewing angle demonstrate the occluded segment and the remainder of the Left circumflex artery which is filled by collaterals. Successful restoration of flow was accomplished by the antegrade technique. Ultimately, the cardiac phase of the CT image would be matched to the cardiac phase of the X-ray data. However, currently the CT images are shown in a pre-selected static cardiac phase; the coronary arteries in the X-ray image will display a periodical motion around the coronary arteries which were segmented from the CT data.

***Plaque evaluation and identification of high risk lesions***

Ulcerated and ruptured plaques as illustrated in Figure 15, and presumed thin cap fibroatheromas can be identified by CTA (see also Figure 4). If ongoing studies prospectively localize ischemic events to vulnerable areas and are accompanied by data supporting stenting these areas, CTA may be used to noninvasively localize the high risk lesion prior to intervention.

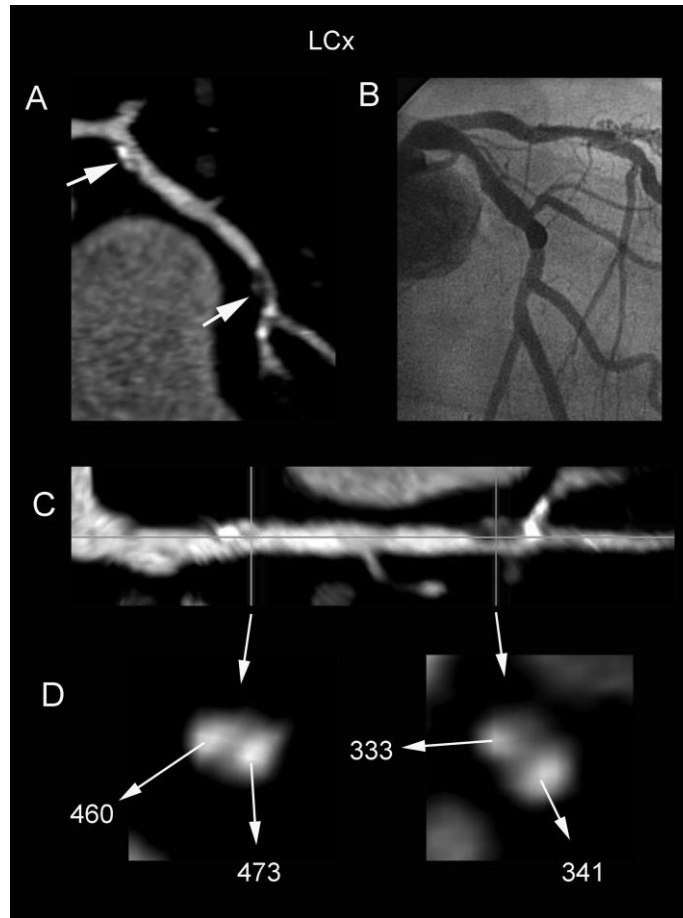


Figure 15: A 52 year old male with prior PCI underwent CTA (A) after presenting with recurrent chest pain. In the proximal LCx (arrow), a complex plaque was noted, containing calcified plaque and a second component extrinsic to the lumen, with density similar to contrast. In the mid LCx, a similar extraluminal density was noted (arrow). CA performed 2 weeks later (B) did not reveal these findings and the mid LCx stenosis was not apparent. Cross sectional analysis (D) of the straightened MPR (C) confirmed the extraluminal densities to be similar to contrast, consistent with plaque rupture at both sites.

Abbreviations: CA= conventional angiography CTA= computed tomographic angiography LCx= left circumflex MPR= multi-planar reconstruction PCI= percutaneous coronary intervention

## **12.7 Conclusions**

That CTA will significantly alter the practice of PCI is abundantly clear; it is still in its relative infancy, with forthcoming technologic advances likely to accelerate the pace of change. The prerequisite human ingredient is a change in mind set, an acknowledgement that the traditional reliance on catheter angiography is limiting, despite the decades of data accumulated in the catheterization laboratory. Had IVUS been available from the very beginning angiography, there is little doubt that it would have been the gold standard. CTA provides the opportunity to incorporate the unique insights offered by IVUS into a universally available noninvasive tool which can now be brought directly into the catheterization laboratory. The likely outcome is transformation of the catheterization laboratory into a streamlined interventional suite, utilizing fused CTA and CCA data in an interactive format.

**References**

[Meijboom08] Meiboom WB, Meijs MFL, Schuijf JD, Diagnostic accuracy of 64-slice computed tomography coronary angiography: A prospective, multicenter, multivendor study, *J. Am Coll Cardiology* 2008;52:2135-144

[Hech07] Hecht HS, Roubin G, Usefulness of Computed Tomography Guided Percutaneous Coronary Intervention, *Am. J. of Cardiology* 2007;99:871-875

[Hendel06] Hendel RC, Patel MR, Kramer CM, et al. ACCF/ACR/SCCT/SCMR/ASNC/NASCI/SCAI/SIR 2006 appropriateness criteria for cardiac computed tomography and cardiac magnetic resonance imaging: a report of the American College of Cardiology Foundation Quality Strategic Directions Committee Appropriateness Criteria Working Group, American College of Radiology, Society of Cardiovascular Computed Tomography, Society for Cardiovascular Magnetic Resonance, American Society of Nuclear Cardiology, North American Society for Cardiac Imaging, Society for Cardiovascular Angiography and Interventions, and Society of Interventional Radiology. *J Am Coll Cardiol* 2006;48:1475-97.1.Maruyama T,

[Motoyama08] Motoyama S, Anno H, Sarai M, Sato T, Sanda Y, et al. Noninvasive coronary angiography with a prototype 256-row area detector computed tomography system: comparison with conventional invasive coronary angiography. *J Am Coll Cardiol* 2008;51:773-5.

[Takada06] Takada M, Hasuike T, et al. Radiation dose reduction and coronary assessability of prospective electrocardiogram-gated computed tomography coronary angiography. Comparison with retrospective electrocardiogram-gated helical scan. *J Am Coll Cardiol* 5. Caussin C, Larchez C, Ghostine S., et al. Comparison of coronary minimal lumen area quantification by sixty-four-slice computed tomography versus intravascular ultrasound for intermediate stenosis. *Am J Cardiol* 2006;98:871-6.

[Caussin06] Caussin C, Larchez C, Ghostine S., et al. Comparison of coronary minimal lumen area quantification by sixt-four-slice computed tomography versus intravascular ultrasound for intermediate stenosis. *Am .J. Cardiol* 2006;98:871-6.

[Okabe08] Okabe T, Weigold WG, Mintz GS, et al. Comparison of intravascular ultrasound to contrast-enhanced 64-slice computed tomography to assess the significance of angiographically ambiguous coronary narrowings. *Am J Cardiol* 2008;102:994-1001.

[Pundziute08a] Pundziute G, Schuijf JD, Jukema JW, et al. Evaluation of plaque characteristics in acute coronary syndromes: non-invasive assessment with multi-slice computed tomography and invasive evaluation with intravascular ultrasound radiofrequency data analysis. *Eur Heart J* 2008;

[Springer08] Springer I, Dewey M. Comparison of multislice computed tomography with intravascular ultrasound for detection and characterization of coronary artery plaques: A systematic review. *Eur J Radiol* 2008.

[Pundziute08b] Pundziute G, Schuijf JD, Jukema JW, et al. Head-to-head comparison of coronary plaque evaluation between multislice computed tomography and intravascular ultrasound radiofrequency data analysis. *J Am Coll Cardiol Intv* 2008;1:176–82

[Thompson06] Thompson RC, Cullom SJ. Issues regarding radiation dosage of cardiac nuclear and radiography procedures. *J Nucl Cardiol* 2006;13:19–23.

[Fleischmann 98] Fleischmann KE, Hunink MG, Kuntz KM, Douglas PS. Exercise echocardiography or exercise SPECT imaging? A meta-analysis of diagnostic test performance. *JAMA* 1998;280:913–20.

[Mollet05] Mollet NR, Hoye A, Lemos PA, et al. Value of preprocedure multislice computed

tomographic coronary angiography to predict the outcome of percutaneous recanalization of chronic total occlusions. *Am J Cardiol* 2005;95:240–3

[Okuyama08] Okuyama T, Ehara S, Shirai N, et al. Usefulness of three-dimensional automated quantification of left ventricular mass, volume, and function by 64-slice computed tomography. *J Cardiol*. 2008 Dec;52(3):276-84.

[Spoeck08] Spoeck A, Bonatti J, Friedrich GJ, et al. Evaluation of left ventricular function by 64-multidetector computed tomography in patients undergoing totally endoscopic coronary artery bypass grafting. *Heart Surg Forum*. 2008;11(4):E218-24.

[Cristoforetti07] Cristoforetti A, Faes L, Ravelli F, et al. Isolation of the left atrial surface from cardiac multi-detector CT images based on marker controlled watershed segmentation. *Med Eng Phys*. 2008 Jan;30(1):48-58. Epub 2007 Mar 27.

[Sun05] Sun W, Qetin M, Chan R, Reddy V, et al. Segmenting and tracking the left ventricle by learning the dynamics in cardiac images. *Inf Process Med Imaging*. 2005;19:553-65.

[Lynch06] Lynch M, Ghita O, Whelan PF, Left-ventricle myocardium segmentation using a coupled level-set with a priori knowledge. *Comput Med Imaging Graph*. 2006 Jun;30(4):255-62.

[Zheng08] Zheng Y, Barbu A, Georgescu B, et al. Four-chamber heart modeling and automatic segmentation for 3-D cardiac CT volumes using marginal space learning and steerable features. *IEEE Trans Med Imaging*. 2008 Nov;27(11):1668-81.

[Ecabert08] Ecabert O, Peters J, Schramm H, Lorenz C, et al. Automatic model-based segmentation of the heart in CT images. *IEEE Trans Med Imaging*. 2008 Sep;27(9):1189-201.

[Wijesooriya08] Wijesooriya K, Weiss E, Dill V, et al. Quantifying the accuracy of automated structure segmentation in 4D CT images using a deformable image registration algorithm. *Med Phys.* 2008 Apr;35(4):1251-60.

[Fleureau07] Fleureau J, Garreau M, Boulmier D, Hernández A, 3D multi-object segmentation of cardiac MSCT imaging by using a multi-agent approach. *Conf Proc IEEE Eng Med Biol Soc.* 2007;2007:6004-7.

[Renno06] Renno MS, Shang Y, Sweeney J, Dossel O, Segmentation of 4D cardiac images: investigation on statistical shape models. *Conf Proc IEEE Eng Med Biol Soc.* 2006;1:3086-9.

[Lorenz06] Lorenz C, von Berg J, A comprehensive shape model of the heart. *Med Image Anal.* 2006 Aug;10(4):657-70. Epub 2006 May 18.

[Assen08] van Assen HC, Danilouchkine MG, Dirksen MS, et al. A 3-D active shape model driven by fuzzy inference: application to cardiac CT and MR. *IEEE Trans Inf Technol Biomed.* 2008 Sep;12(5):595-605.

[Cho05] Cho J, Benkeser PJ. Cardiac segmentation by a velocity-aided active contour model. *Comput Med Imaging Graph.* 2006 Jan;30(1):31-41. Epub 2005 Dec 27.

[Higging90] Higgins WE, Chung N, Ritman EL, Extraction of left-ventricular chamber from 3-D CT images of the heart. *IEEE Trans. Med. Imag.* 9(4):384-394, 1990.

[Redwood05] Redwood AB, Camp JJ, Robb RA, Semiautomatic segmentation of the heart from CT images based on intensity and morphological features. *Proc. SPIE Med. Imag.* 5747: 1713-1719, 2005.

[Marquering05] Marquering HA, Dijkstra J, de Koning PJ, Stoel BC, Reiber JH, Towards quantitative analysis of coronary CTA. *Int J Cardiovasc Imaging*. 2005 Feb;21(1):73-84.

[Saur08] Saur SC, Alkadhi H, Desbiolles L, et al. Automatic detection of calcified coronary plaques in computed tomography data sets. *Med Image Comput Comput Assist Interv Int Conf Med Image Comput Comput Assist Interv*. 2008;11(Pt 1):170-7.

[Isgum07] Isgum I, Rutten A, Prokop M, van Ginneken B, Detection of coronary calcifications from computed tomography scans for automated risk assessment of coronary artery disease. *Med Phys*. 2007 Apr;34(4):1450-61.

[Horiguchi07] Horiguchi J, Fujioka C, Kiguchi M, et al. Soft and intermediate plaques in coronary arteries: how accurately can we measure CT attenuation using 64-MDCT? *AJR Am J Roentgenol*. 2007 Oct;189(4):981-8.

[Bousse06] Bousse A, Boldak C, Toumoulin C, et al. Coronary extraction and characterization in multi-detector computed tomography, *ITBM-RBM*, 27(5-6):217-226, November-December 2006

[Fallavollita06] Fallavollita P, Cheriet F, Towards an automatic coronary artery segmentation algorithm. *Engineering Conference Proceedings IEEE Engineering in Medicine and Biology Society* 2006:3037-40

[Fallavollita08] Fallavollita P, Cheriet F, Optimal 3D reconstruction of coronary arteries for 3D clinical assessment, *Computerized Medical Imaging and Graphics*, 32(6):476-487, September 2008

[Mueller08] Mueller D, Maeder A, Robust semi-automated path extraction for visualising stenosis of the coronary arteries. *Comput Med Imaging Graph*. 2008 Sep;32(6):463-75.

[Zambal08] Zambal S, Hladuvka J, Kanitsar A, Buehler K. Shape and Appearance Models for Automatic Coronary Artery Tracking. MICCAI 2008 Workshop

[Frangi98] Frangi AF, Niessen WJ, Vincken KL, Viergever MA, Multiscale vessel enhancement filtering. Proc MICCAI'98:130-137

[Metz08] Metz CT, Schaap M, van Walsum T, et al. 3D Segmentation in the Clinic: A Grand Challenge II - Coronary Artery Tracking. MICCAI 2008 workshop

[Kanitsar02] Kanitsar A, Fleischmann D, Wegenkittl R, et al. - CPR Curved Planar Reformation. VIS '02: IEEE Proc. Conf. Visualization '02, Boston, Ma, USA.

[Garcia07] Garcia JA, Eng MH, Wink O, et al. - Clinical Review: Image Guidance of Percutaneous Coronary and Structural Heart Disease Interventions Using a Computed Tomography and Fluoroscopy Integration. Vascular Disease Management, 4(3), pp 89-97, May 2007.

[Hecht08] Hecht HS, Applications of Multislice Coronary Computed Tomography Angiography to Percutaneous Coronary Intervention: How did we ever do without it?, Cath and Cardiovasc Interven 71:490-503, 2008.

[Otsuka08], Otsuka M, Sugahara S, Umeda K, et al. Utility of multislice computed tomography as a strategic tool for complex percutaneous coronary interventions. International Journal Cardiovascular Imaging 24:201-210, 2008.

[Russakoff05] Russakoff DB, Rohlfing T, Mori K, et al. Fast generation of digitally reconstructed radiographs using attenuation fields with application to 2D-3D image registration, Medical Imaging, IEEE Transactions on, Volume 24, Issue 11, Nov. 2005 Page(s):1441 – 1454

[Tobis07] Tobis J, Azarbal B, Slavin L, Assessment of intermediate severity coronary lesions in the catheterization laboratory. *J Am Coll Cardiol* 2007;49:839–48.

[Weese97] Weese J, Buzug TM, Lorenz C, Fassnacht C, An approach to 2D/3D registration of a vertebra in 2D X-ray fluoroscopies with 3D CT images. *CVRMed* 1997: 119-128

[Sra07] Sra J, Narayan G, Krum D, et al. Computed tomography-fluoroscopy image integration-guided catheter ablation of atrial fibrillation. *J Cardiovasc Electrophysiol*. 2007 Apr;18(4):409-14.

[Knecht08] Knecht S, Skali H, O'Neill MD, et al. Computed tomography-fluoroscopy overlay evaluation during catheter ablation of left atrial arrhythmia. *Europace*. 2008 Aug;10(8):931-8.

[Turgeon05] Turgeon GA, Lehmann G, Guiraudon G, et al. 2D-3D registration of coronary angiograms for cardiac planning and guidance. *Medical Physics* 32(12) (2005) 3737-3749

[Garcia08] Garcia JA, Bhakta S, Kay J, et al. On-line multi-slice computed tomography interactive overlay with conventional X-ray: A new and advanced imaging fusion concept. *Int J Cardiol*. 2008 Jan 28: 18234371

## Legends

- Figure 1: Example of model-based fully automatic segmentation of the main cardiac structures from a CTA dataset.6
- Figure 2: Example of the segmented heart from a CTA volume. A slice from the original CTA scan (A), the same slice after segmenting the heart (B), and a color coded volume rendering of the segmented heart (B). .....7
- Figure 3: Example of a vessel enhanced image. The left frame shows the original CT data. The right frame shows the same dataset after a vesselness filter was applied. In the center of the volume some of the major coronary arteries are visible. ....8
- Figure 4: Example of different MPR's and Quantitative CTA analysis. ....9
- Figure 5: In room presentation of CTA data using volume rendering and MPR visualization techniques.....14
- Figure 6: Example of a digitally reconstructed radiograph (DRR) based on a segmented CTA dataset. ....15
- Figure 7: Example of visualizing the CT based coronary tree from different viewing angles and the corresponding C-arm gantry configuration.....16
- Figure 8: Example of a registration based on the coronary arteries.....18
- Figure 9: CTA guided PCI paradigm. Abbreviations: CABG= coronary artery bypass grafting. CTA= computed tomographic angiography. FFR= fractional flow reserve. IVUS= intravascular ultrasound. LM= left main. MLA= minimum lumen area. PCI= percutaneous coronary intervention. V= vessel. ....19
- Figure 10: In a symptomatic 64 year old male with prior LAD stent, CTA curved MPR of the LAD (A) revealed significant diffuse narrowing from the LAD ostium to the stent, with only mild narrowing evident on the corresponding CA (B). Cross sectional analysis (D) of the straightened MPR (C) demonstrated significantly reduced MLA of 2.9 mm<sup>2</sup>, confirmed by IVUS (D), and followed by PCI.....20
- Figure 11: An 80 year old female with increasing dyspnea and prior LAD stenting was evaluated. CTA revealed severe hypodensity consistent with significant in-stent restenosis (A, top) that appeared to be only moderately severe on CA (A, bottom). Cross sectional analysis (C) of the straightened MPR (B) in 2 adjacent areas of the stent demonstrated the hypodensity characteristic of neointimal hyperplasia (arrows), as well as severely decreased MLA, confirmed by IVUS (C). PCI was performed. In-stent MLA calculation is rarely possible. Blooming artifact from the dense stent material almost always precludes accurate measurement; ISR is diagnosed by qualitative density levels. ....21

Figure 12: In a 66 year old male with increasing angina, subtotal LAD occlusion (arrow) was noted on the CTA (A, left) and on the CA (A right). Proximal and distal stent landing zones, 23.6 mm apart, were chosen on the straightened MPR (B). Mean luminal diameters for the landing zones were determined by cross sectional analysis to be 4.4 and 3.1 mm, respectively (C). PCI was performed using a 25 mm x 3.5 mm stent, with post inflation of the proximal segment to 4.5 mm to achieve full apposition. ....22

Figure 13: Selective angiography demonstrated flush occlusion of the LAD with partial collateral filling from the RCA (A) in a symptomatic 65 year old woman with anterior ischemia. After 6 months of persistent symptoms, CTA guided intervention was planned. Curved MPR readily visualized the occluded LAD segment (B). CTA mapping (TrueView, Philips) of the left coronary artery and all its branches (C) was imported to the catheterization laboratory monitor and electronically linked to the C-arm. The C-arm was rotated, with accompanying automatic rotation of the TrueView map to the angle predetermined by the CTA to best demonstrate the origin and course of the chronic total occlusion without overlapping branches. Simultaneous injection of the right and left coronary arteries (D) was performed. With TrueView guidance, the guidewire was introduced to the precise origin of the flush occlusion, followed by successful recanalization and further stenting of the distal vessel 6 weeks later (E) .....24

Figure 14: Fusion of CT and X-ray images (roadmapping) A and the corresponding MPR (B). .....25

Figure 15: A 52 year old male with prior PCI underwent CTA (A) after presenting with recurrent chest pain. In the proximal LCx (arrow), a complex plaque was noted, containing calcified plaque and a second component extrinsic to the lumen, with density similar to contrast. In the mid LCx, a similar extraluminal density was noted (arrow). CA performed 2 weeks later (B) did not reveal these findings and the mid LCx stenosis was not apparent. Cross sectional analysis (D) of the straightened MPR (C) confirmed the extraluminal densities to be similar to contrast, consistent with plaque rupture at both sites. ....26